crystals

MDPI

Article

Colloidal Nanocrystalline Semiconductor Materials as Photocatalysts for Environmental Protection of Architectural Stone

Francesca Petronella [1,†], Antonella Pagliarulo [1,†,‡], Marinella Striccoli [1], Angela Calia [2], Mariateresa Lettieri [2], Donato Colangiuli [2], Maria Lucia Curri [1] and Roberto Comparelli [1,*]

1 CNR-IPCF, Consiglio Nazionale delle Ricerche, Istituto per i Processi Chimici e Fisici, U.O.S. Bari 70126, Italy; f.petronella@ba.ipcf.cnr.it (F.P.); antonella.pagliarulo@durham.ac.uk (A.P.); m.striccoli@ba.ipcf.cnr.it (M.S.); lucia.curri@ba.ipcf.cnr.it (M.L.C.)

2 CNR-IBAM, Consiglio Nazionale delle Ricerche Istituto per i Beni Archeologici e Monumentali, Lecce 73100, Italy; a.calia@ibam.cnr.it (A.C.); mt.lettieri@ibam.cnr.it (M.L.); d.colangiuli@ibam.cnr.it (D.C.)

* Correspondence: r.comparelli@ba.ipcf.cnr.it or roberto.comparelli@cnr.it; Tel.: +39-080-5442027

† These authors contributed equally to this work.

‡ Present address: Department of Chemistry Durham University United Kingdom.

Academic Editor: Helmut Cölfen

Received: 2 November 2016; Accepted: 14 January 2017; Published: 20 January 2017

Abstract: Rod-shaped TiO_2 nanocrystals (TiO_2 NRs), capped by oleic acid molecules (OLEA), were synthesized with controlled size, shape and surface chemistry by using colloidal routes. They were investigated for application as coating materials for preserving architectural stone of monumental and archaeological interest, in consideration of their self-cleaning and protection properties. For this purpose, two different deposition techniques, namely casting and dipping, were tested for the application of a nanocrystal dispersion on a defined stone type, as a relevant example of porous calcarenites, namely the *Pietra Leccese*, a building stone widely used in monuments and buildings of cultural and historic interest of the Apulia region (Italy). The physical properties of the stone surface were investigated before and after the treatment with the prepared nanostructured materials. In particular, colour, wettability, water transfer properties and stability of the coating were monitored as a function of time and of the application method. The self-cleaning properties of the TiO_2 NRs coated surfaces were tested under simulated and real solar irradiation. The obtained results were discussed in the light of the specific surface chemistry and morphology of TiO_2 NRs, demonstrating the effectiveness of TiO_2 NRs as an active component in formulations for stone protection.

Keywords: colloidal nanocrystals; photocatalysis; limestone; coating; self-cleaning; hydrophobicity; stone protection

1. Introduction

Preventive conservation of stone buildings and monuments represents a crucial challenge, due to peculiar relevance of the extraordinary cultural heritage in many countries. Aging, weather exposure and environmental pollution significantly threaten the exceptional legacy represented by artistic and historical monuments and buildings that possess unique social, historical, cultural and economic value, since they are relevant assets of the tourism-related industry [1,2].

The causes of deterioration of historical immovable objects are multifold, therefore innovative treatments, effective in providing multiple answers, would be amenable.

In this perspective, the monument surface should be protected by multifunctional coatings, able to comply several fundamental conditions that make such a multidisciplinary task extremely challenging. Coatings are often required to be hydrophobic, in order to prevent water infiltration; in addition, they

should be: (i) compatible with the substrate and reversible; (ii) resistant to weathering and to UV fraction of solar spectrum; (iii) able to preserve the aesthetic aspect of the monuments; and (iv) based on safe solvents and at neutral pH [3].

Thus far, protection of stone materials was mainly achieved by means of polymeric coatings, such as acrylic, fluorinated and alkoxysilanes. Recent studies, however, highlighted some drawbacks regarding the loss of adhesion and effectiveness, caused by temperature variations, solar irradiation and atmospheric pollutants. Acrylic resins undergo photo-oxidative irreversible modifications that make the coating hard to remove [4]. Moreover, chemical aging of acrylic-based polymers due to photo-oxidative reactions leads to the formation of oxidized species such as c-lactones, which cause the polymeric coating to yellow, thus affecting the aesthetic features of the treated surfaces [5].

Recently, a fluoro-modified PLA (PolyLactic Acid) was proposed by Pedna et al. as protective coating that can be obtained from renewable source, being particularly attractive because of its reversibility, its high hydrophobicity and its ability to preserve the surface aesthetics [6].

Alternatively, fluorinated polymers are very interesting because of their photo-stability, water repellence and anti-vegetative properties. However, while silicon-based and acrylic-based coatings bind at the monument surface via covalent bond and dipole bond, respectively, fluorinated polymers can stick to monument surfaces only via weak van der Waals forces. For this reason, copolymers or blends of fluoropolymers with acrylic or silicon polymers were investigated in order to convey hydrophobicity to monument surfaces and to obtain an improved adhesion [3].

Fluorinated coatings were tested as stone protective agents, being also available as many commercial products used as anti-graffiti [7,8]. Nonetheless, these products do not possess self-cleaning ability. Self-cleaning properties can be achieved by integrating suitable photocatalytic nanomaterials in polymer-based coatings, so they can convey their ability to perform photodegradation of pollutants. In this perspective, TiO_2 is receiving increasing attention due to its well-known photocatalytic activity. Such a property is exploited to convey self-cleaning, antimicrobial, and [9] anti-odour functions to window glasses, pavements, walls, and roofs [10] as well as to ceramic materials [11], being also responsible for the variation of the surface wettability, resulting in super-hydrophobic or super-hydrophilic surfaces thus increasing their self-cleansing capacity [12,13].

The photocatalytic process occurs when TiO_2 is irradiated with photons having energy higher than or equal to its band gap energy, generating photo-electrons (e^-) and photo-holes (h^+) [14] charges can migrate to the photocatalyst surface where they can react with adsorbed electron donors or electron acceptors. In this step, strongly reactive radicals, potentially able to destroy both organic and inorganic compounds, are generated [15].

The use of nanosized TiO_2 has been recently investigated in polymeric matrices with promising results in order to obtain multifunctional coatings for application to stone materials. Cappelletti and co-workers compared the performance of a commercially available polysiloxane with a mixture of nanosized TiO_2 and the polysiloxane, showing that TiO_2 nanoparticles in the polymer are responsible for the increase of surface roughness that provides a super-hydrophobic character to the coating, thus resulting in enhanced effectiveness in reducing salt formation [16]. Studies were also performed on mixtures of nanostructured TiO_2 and fluorinated polymers, which assessed the simultaneous photocatalytic and hydrophobic properties of the coatings applied on limestone substrates [17,18]. A self-cleaning coating, effective under visible light, was obtained by including a colloidal dispersion of a TiO_2 and Ag in a sol of silica oligomers with the assistance of n-octylamine as surfactant [19]. Further, a visible light active self-cleaning coating was also achieved by combining TiO_2 sol with Au nanoparticles [20]. Other studies investigated the role played by the morphology of TiO_2 nanoparticles in improving the self-cleaning and the hydrophobic properties as well as the consolidating effect of TiO_2-SiO_2 nanocomposite based coatings on limestone or dolostone [21,22]. In order to minimize the presence of cracks, which are detrimental to the photocatalytic activity of the coatings, Pinho et al. prepared a nanocomposite made of TiO_2 nanoparticles dispersed into a silica matrix that was then

deposited onto limestone, resulting in a stable coating that, however, suffered the limitation of reduced photoactivity, even under UV radiation [23].

Here, TiO_2 nanocrystals with a rod-like geometry, capped by oleic acid molecules (OLEA), hereinafter referred to as TiO_2 NRs, are proposed as a functional material. The TiO_2 NRs can be effectively processed and applied as component in composite materials or, like in this work, dispersed in a solvent to convey both self-cleaning and protective properties to an example of porous calcarenitic stones, namely the *Pietra Leccese* (PL), which is characteristic of the South of Italy. In the reported approaches, photoactive nanomaterials were mainly deposited on large surfaces as a composite coating, formed of a suitable host polymer incorporating the active nanomaterial [24]. Here, we exploited the unique processability of OLEA coated TiO_2 NRs, deriving from their peculiar surface chemistry, to disperse the nanoparticles in organic solvents. The resulting dispersions were optically clear indicating no aggregation of the TiO_2 NRs, and could be directly applied to treat the PL stone surface. Such an approach has been selected not only because it allows a prompt evaluation of the nanomaterial properties as a functional active component for stone protection, but also because it could offer, in principle, several advantages. In fact, when TiO_2 NRs are freely dispersed and not embedded in any polymeric matrix, their surface is fully available to interact with the PL stone. Conversely, when TiO_2 nanoparticles are embedded in a host matrix, only a small fraction of the TiO_2 is available as active material exposed at the surface of the stone, with a consequent, anticipated drop of performance. Moreover, a polymeric matrix could undergo, in most of cases, degradation phenomena due to the photooxidizing action of TiO_2. Finally, the incorporation of TiO_2 NRs in a suitable polymeric matrix generally requires ligand exchange procedures that can imply aggregation phenomena with a resulting decrease of surface active sites. Such aggregation can be, in fact, prevented maintaining the pristine ligand of TiO_2 NRs. Finally, the TiO_2 NRs were selected for their unique chemical-physical characteristics and the well-established photocatalytic activity in aqueous media [25–27].

Thanks to their nanosize and anisotropic shape, TiO_2 NRs possess a high surface area, hence, a high amount of surface active sites [28]. In addition, the specific geometry limits the charge carriers recombination because e^-/h^+ can, in principle, locate in distal part of anisotropic nanostructure, thus ensuring an efficient charge separation [29]. Furthermore, TiO_2 NRs are synthesized in anatase phase, which is reported to be the most photoactive phase of TiO_2 [30]. Finally, the surface of TiO_2 NRs is coordinated by OLEA molecules, able to convey, in principle, a hydrophobic character to the PL stone surface once deposited, increasing, at the same time, the photocatalytic activity due to the stabilization of the photogenerated holes on TiO_2 provided by the OLEA molecules at the surface [31].

The effect of the deposition procedure on PL stone surface, namely casting and dipping, was investigated, as a function of the amount of applied OLEA coated TiO_2 NRs, by studying the chemical-physical properties of the treated stone and, ultimately, their self-cleaning ability and hydrophobic properties.

The chemical-physical characterization of the treated samples was carried out to monitor the basic requirements that a component in a protective formulation needs to fulfil for the application to historically and artistically relevant building materials. For this purpose, colour variation measurements were performed in order to monitor the aesthetical features of the PL surface upon TiO_2 NR treatment. Static contact angle measurements assessed wettability of the treated stone, while water absorption tests were carried out to evaluate the protection ability of the coatings against water penetration into the stone. Water vapour transfer properties of the coated stone were assessed by a permeability test. The stone samples, treated with TiO_2 NRs dispersion, showed that the application technique affected the final hydrophobic properties, while the applied coatings preserved aesthetic characteristics of the PL and remarkably conveyed to the PL the self-cleaning ability of the photocatalytically active TiO_2 NRs.

2. Results and Discussion

2.1. TiO_2 NR Characterization

Before proceeding with the transmission electron microscopy (TEM) and Fourier transform infrared spectroscopy in attenuated total reflectance mode (FT-IR-ATR) characterization, the as synthesized TiO_2 NRs were washed five times according to the procedure described in the Experimental Section to remove the excess of uncoordinated OLEA molecules.

Figure 1a, reports the typical TEM micrograph of the obtained sample, which is found to consist of rod-shaped and high aspect ratio nanocrystals of about 3 nm in diameter and with an average length of 18 nm. The TiO_2 structures result anatase in phase and with a surface area of 240 ± 5 m^2/g [28,32].

The FT-IR-ATR spectrum of TiO_2 NRs in the region 4000–600 cm^{-1} is reported in Figure 1b. Above 2000 cm^{-1}, the TiO_2 NR samples exhibit the antisymmetric and symmetric C–H stretching vibrations (at 2920 and 2850 cm^{-1}, respectively) of the $–CH_2–$ groups in the hydrocarbon chain of OLEA. The shoulder at 2960 cm^{-1} can be associated with the asymmetric stretching of the terminal $–CH_3$ group of the alkyl chain. Accordingly, the typical O–H broad stretching band centred at 3000 cm^{-1}, which is distinctive of OLEA dimers, is detectable. The wide absorption below 950 cm^{-1} is ascribable to the characteristic vibration of the inorganic Ti–O–Ti network in TiO_2. Interestingly, the weakening of the typical C=O stretching vibration suggested that the –COOH groups of OLEA are involved in the coordination of TiO_2 NR surface [32]. Therefore, residual OLEA molecules are present on TiO_2 NR surface as coordinating agent. Further, such OLEA at TiO_2 NR surface can play a beneficial role in photocatalysis allowing to further stabilize the photo-induced excited state of TiO_2 nanocrystals, as already demonstrated by a EPR study [31].

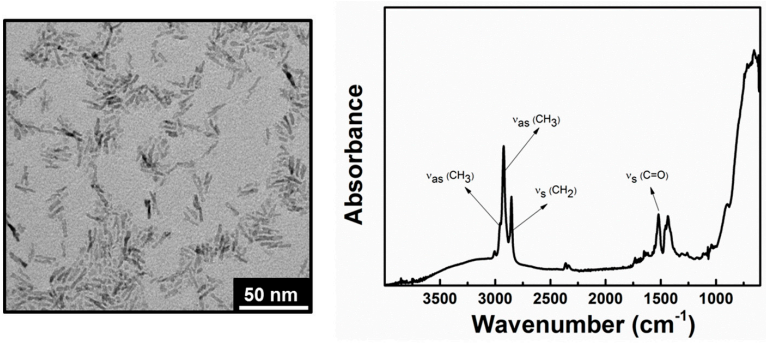

(a) (b)

Figure 1. (**a**) Transmission electron microscopy image of a typical TiO_2 NR sample. (**b**) FT-IR-ATR spectra of TiO_2 NRs in the 4000–600 cm^{-1} region after the purification step.

2.2. Characterization of the TiO_2 NR Treated Samples

Defined amounts of TiO_2 NR dispersion were cast on the PL stone samples and the solvent let to evaporate. Such a method allowed controlling the amount of TiO_2 NRs applied on the stone, thus, simulating a brush type of application. The amount of TiO_2 NRs per surface unit on the stone was determined by weighing with an analytical balance with readability up to 0.01 mg (Table 1).

The dipping procedure relied on the immersion of the PL sample in a chloroform dispersion of TiO_2 NRs. In this case, dispersions at different TiO_2 NR content were investigated (Table 1). Such a method, although in principle not relevant for application on buildings or monuments, could, be considered for application on small artefacts or as a conditioning treatment to be applied on the stone blocks to be used in buildings or on artefacts. The amount of TiO_2 NRs on the stone was below the detection limit of the analytical balance. Therefore, the concentration of the solution used for the deposition has been reported in Table 1.

Table 1. Experimental conditions for the deposition of TiO_2 NRs on PL samples by casting and dipping; colorimetric variation of the surface of the stone after the treatment (ΔE*); and static contact angles measurements (α) after the treatments with TiO_2 NRs.

Sample	TiO_2	ΔE*	α (°) ± sd
PL1c	0.48 mg/cm^2	3.71	134 ± 6
PL2c	0.32 mg/cm^2	3.64	132 ± 8
PL3c	0.03 mg/cm^2	1.57	144 ± 5
PL1d	0.02 M	2.34	142 ± 3
PL2d	0.01 M	1.32	134 ± 6
PL3d	0.005 M	1.95	135 ± 4
OLEA	0.016 mg/cm^2	1.01	32 ± 13

It is worth noting that, in the field of cultural heritage material protection and restoration, the preservation of the original aesthetic features of buildings and monuments of historical or artistic interest is a fundamental requirement.

The visual appearance of the PL sample, after the treatment, either by casting and dipping did not show any significant colour variation in comparison with an untreated sample, as reported in Figure 2a,b.

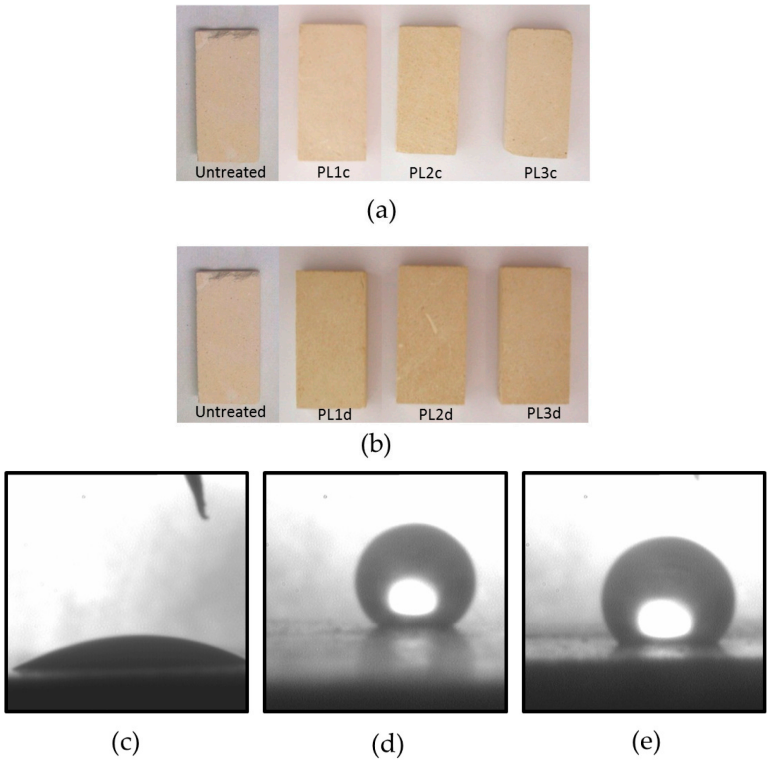

Figure 2. Picture of the stone samples treated with increasing amount of TiO_2 NRs by: casting (**a**); and dipping (**b**); in both cases compared with the untreated PL sample (**c**). Static contact angle picture of the PL sample treated with: OLEA (**c**); PL3c (**d**); and PL3d (**e**).

Table 1 shows the values of the colour variation ΔE* measured for each PL sample, after the treatment indicating that the application of TiO_2 NRs did not, in any case, significantly affect the visual appearance of the treated stones. Nonetheless, it can be observed that the highest colour variations were recorded in the case of application by casting on the surface of PL1c and PL2c samples, yielding similar ΔE* values of 3.71 and 3.64, respectively. At the lowest amount of TiO_2 NRs per surface unit applied in the case of PL1c, a notably lower value of ΔE* was recorded. Samples treated by dipping

yielded less significant colour changes. The maximum value of ΔE*, namely 2.34, was measured on the surface of the PL1d sample, while colour changes resulting from dipping of PL2d and PL3d samples were lower and comparable to the value measured in the case of PL1c. Nonetheless, evidence of the presence of TiO_2 NRs on the PL surface is provided by the diffuse reflectance spectra of the representative samples PL3c and PL3d, compared with the diffuse reflectance spectra of an untreated PL sample (Figure 3b).

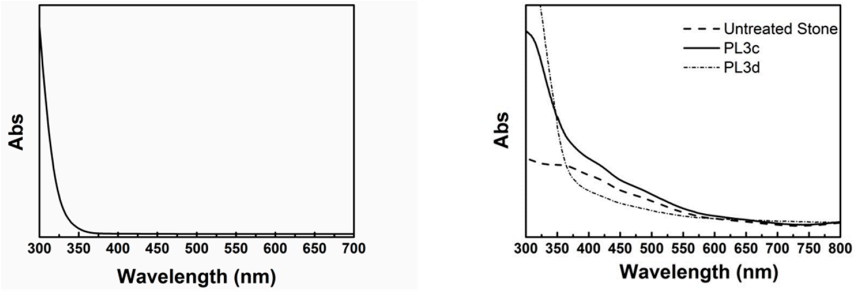

(a) (b)

Figure 3. (**a**) Absorption spectrum of a chloroform solution of TiO_2 NRs; and (**b**) reflectance spectrum of a *Pietra Leccese* sample PL3c and PL3d before and after TiO_2 NR deposition.

The spectra of PL3c and PL3d exhibit a significant absorption increase in the region below 350 nm, consistent with the typical absorption spectrum of TiO_2 NRs dispersed in a solvent reported in Figure 3a. Such an increase in absorbance was not observed in the diffuse reflectance spectrum of the untreated PL sample.

Water is recognised as one of the main causes of damage for stone materials [33,34]. Therefore, the ability of a coating material to act as a protecting layer against water absorption is a critical issue worth exploring.

In this perspective, static contact angle measurements were performed in order to investigate the wettability of the treated PL surfaces. Experimental results, reported in Table 1, pointed out a static contact angle value higher than 130° for all the TiO_2 NR treated PL samples, thus proving their hydrophobic character. Such evidence is further highlighted in the pictures in Figure 2d,e that show the static contact angle on PL3c and PL3d sample surfaces. Remarkably, no contact angle measurements could be carried out on an untreated PL sample, as the water droplet used for the measure was completely absorbed by the PL sample due to its high porosity, known to be around 40% [35].

The hydrophobic behaviour conveyed by the TiO_2 NR treatment to the PL surface can be accounted for by the specific surface chemistry of TiO_2 NRs, coordinated by the carboxylic moiety of OLEA. Indeed, the OLEA hydrophobic chain points outward, thus providing a hydrophobic character to the TiO_2 nanocrystals and, accordingly, to the nanostructure treated stone surface [32].

Surprisingly, the treatment of the PL stone surface with the bare OLEA solution was not able to convey as well the hydrophobic character, as demonstrated by the static contact angle measured on a sample where a chloroform solution of OLEA was cast (Figure 2d). The contact angle measure in this case was, in fact, only 32° thus accounting for a hydrophilic behaviour, as pointed out in Figure 2d. This feature can be reasonably explained considering that OLEA molecules, when not coordinated to the TiO_2 NR surface, can randomly orient on the stone sample. Therefore, the assumption is that only the presence of TiO_2 NRs, able to coordinate OLEA molecules to expose the hydrophobic moieties toward the solid–air interface, can be considered responsible for the hydrophobic behaviour of the treated PL surface.

Another critical feature to be considered is the ability to limit penetration of water from outside without hindering the outflow of water vapour from the inner stone towards the surface.

In this regard, water absorption measurements provide useful information on the ability of the coatings to prevent water penetration, thus further assessing the effectiveness of the hydrophobic coating.

The capillary absorption was investigated on the different treated stone samples. In particular, the PL3c and the PL3d samples were selected on the basis of ΔE* and static contact angle values as the most advantageous for the specific properties, having the lowest ΔE* and highest contact angle values, respectively, and being characterized by a suitable trade off of the two values. Both PL3c and PL3d showed a significant decrease of capillary absorption ability. Indeed, as reported in Table 2, water capillary absorption decreased from 86.20 mg/min·cm^2 and 88.9 mg/min·cm^2 in the untreated samples to 0.47 mg/min·cm^2 and 11.06 mg/min·cm^2 in PL3c and PL3d, respectively. In summary, in the PL3c and the PL3d, a decrease of the water absorption of the 87% and 99%, respectively, was found. The difference in terms of amount of water absorption between PL3c and PL3d could be accounted for by the fact that when dipped the sample was completely immersed into the TiO_2 NR dispersion. In this way, a deeper penetration of the TiO_2 NRs could be achieved in the PL3d sample, while, in the case of the PL3c, the TiO_2 NR treatment was applied only to the upper surface of the sample.

Table 2. Water absorption (mg/min·cm^2) as a function of application method for untreated stone specimen and stone specimens treated by casting (PL3c) and dipping (PL3d). The fourth column shows the percentage of WA variation upon the treatment with TiO_2 NRs (Δ %).

Sample	Untreated (mg/min·cm^2)	Treated with TiO_2 NRs (mg/min·cm^2)	Δ (%)
PL3c	86.20	11.06	−87.2
PL3d	88.99	0.47	−99.5

When TiO_2 NR treatment was performed by dipping, for the sample PL3d, the TiO_2 NR dispersion could easily penetrate inside the stone pores. Consequently, the deposition of the TiO_2 NR hydrophobic film is not limited to the stone outer surface, but can also occurs underneath the surface, and inside the pores.

As reported in Table 3, a decrease in water vapour permeability was observed in the case of PL3d, while a slight increase was detected for PL3c. This latter evidence is consistent with what reported in marble samples [36] and in membranes [37], both functionalized with fluorine-based hydrophobic thin coatings. In these reports, the higher permeability in the treated samples was related to a probable lower condensation phenomenon on the hydrophobic pore walls. Consequently, the diffusion rate of water vapour through hydrophobic pores was higher than the diffusion rate through hydrophilic pores. This effect was found neutralized when the polymer layer onto the pore walls was thick enough to reduce the pores' dimensions.

Table 3. Water vapour permeability (g/m^2·24 h) as a function of application method for untreated and the treated samples, either by dipping (PL3d) or casting (PL3c). The fourth column shows the percentage of Water vapour permeability variation upon the treatment with TiO_2 NRs (Δ (%)).

Sample	Untreated (g/m^2·24 h)	Treated with TiO_2 NRs (g/m^2·24 h)	Δ (%)
PL3c	228	248	+8.9
PL3d	331	293	−11.5

The water permeability is also correlated with the stone porosity. In particular, for cement and cement/lime mortars, an increase of the water permeability with the increase of porosity was reported [38]. It is well known that the PL shows a porosity of around 40% with pore size ranging from 10 to 0.3 μm [35]. Accordingly, as the water vapour permeability decreased when the PL stone was treated by dipping for the sample PL3d, it can be suggested that the dipping, in principle, could

affect the total porosity of the PL sample, probably due to the different penetration depth in the stone structure of the nanoparticles during the treatment.

2.3. Photocatalysis Test

Photocatalysis experiments were performed at solid-air interface to investigate the self-cleaning properties of the specimens reported in Table 1 under a solar light simulator. A solution of Methyl Red (MR) in isopropanol was used as model compound to simulate a generic pollutant at the surface of the stone. The MR solution represents a convenient choice because its degradation mechanism was extensively investigated in water solution and it is thus possible to obtain reliable information on the photo-degradation course [25,28]. After treating each stone by casting a defined volume of MR solution, photocatalysis experiments were performed by monitoring total reflectance spectra at scheduled time intervals. To obtain a selective identification of MR signals, the reflectance spectra of the treated stones before MR staining was used as a reference.

Photocatalytic tests were typically carried out for 24 h, following the temporal evolution of the main MR absorption peak at 460 nm. The decolouration percentage over the irradiation period was calculated as reported in Section 3 for all investigated coatings. It is reported as function of irradiation time in Figure 4a,b for the PL samples treated by casting and dipping, respectively.

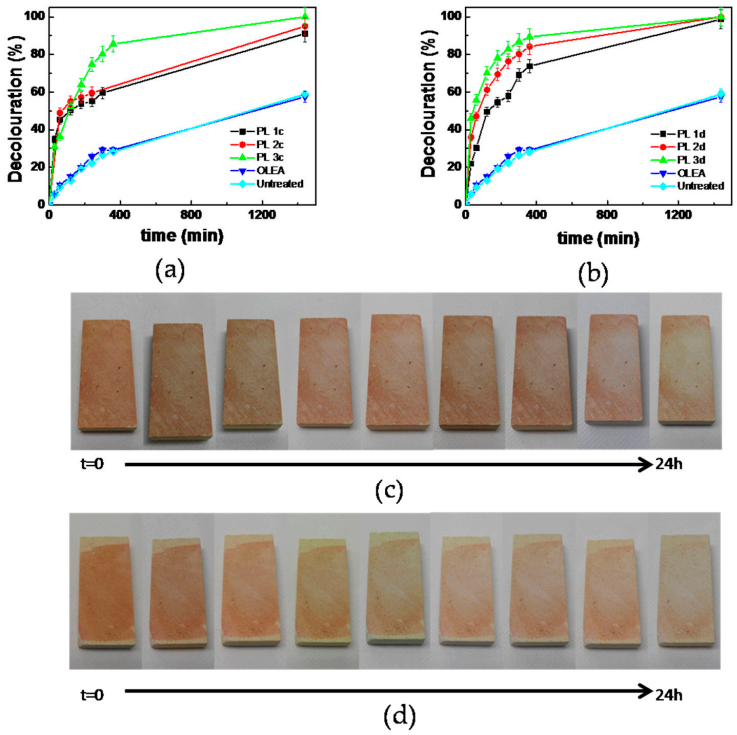

Figure 4. Photocatalytic decolouration of Methyl Red (MR) calculated for all PL samples treated by: casting (**a**); and dipping (**b**) exposed to a solar light simulator for 24 h. An untreated PL sample and a PL sample with OLEA were considered as a reference. Reported data are presented as mean values ± standard deviation obtained from the analysis of two replicates. Visual appearance of samples: PL3c (**c**); and PL3d (**d**) during the photocatalysis experiments. The pictures highlight the effective degradation of MR applied on the treated surface, as indicated by the progressive decolouration of the surface of the stone sample.

The experimental data showed that all the treated specimens were photoactive compared to the untreated PL sample and to the PL sample treated with the solution of OLEA and were able to promote the complete MR decolouration during the 24 h of exposure to the solar light simulator.

In particular, after 4 h, the decolouration percentage was 57% for PL1d specimen, 76% for PL2d and 82% for PL3d. For the treated samples prepared by casting, after 4 h of irradiation by the solar light simulator, the detected decolouration percentage was 55%, 59%, and 74% for samples PL1c, PL2c, and PL3c, respectively. This result points out the remarkable effectiveness of TiO_2 NRs to act as a photocatalyst at solid–air interface under visible light, and suggests that the small fraction of UV light emitted by the solar light simulator can trigger the TiO_2 NRs photocatalytic action.

Therefore, in the case of PL samples functionalized by casting, the photocatalytic activity can be summarized as PL1c < PL2c < PL3c, whereas, in the case of PL sample prepared by dipping, the trend is given by PL1d < PL2d < PL3d. Remarkably, PL3c and PL3d samples, prepared with the most diluted solutions of TiO_2 NRs, were the most photoactive samples under the investigated conditions.

These results can be explained considering that when a low amount of TiO_2 NRs was deposited on the PL sample, a thin film with homogeneous distribution of TiO_2 nanocrystals was obtained, able to maximize the extent of the exposed surface active sites available for the adsorption of the target molecules and for the production of reactive radicals.

Conversely, when TiO_2 NRs were deposited from dispersion at a higher nanoparticle content, a thicker film of NRs formed, thus possibly causing cracks or shrinkage of the structure, with a concomitant loss in its mechanical stability, which negatively affects its photoactivity [39].

Sample PL3d was selected for recycling experiments because it exhibited the highest photoactivity under the investigated conditions. This recycling test consisted in 10 repetitions of the photocatalysis decolouration experiment performed under solar light simulator, in the same conditions illustrated, for an overall irradiation time of 240 h.

The decolouration percentage experimental data, reported in Figure 5, highlight that after each 24-h repetition, almost 100% decolouration was achieved. The PL3d sample still showed significant photoactivity after a high number of repetitions, revealing a suitable candidate for outdoor experiments. Indeed, PL3d was stained with the solution of MR and then exposed outdoor for one week. The decolouration of MR was monitored by performing diffuse reflectance spectroscopy measurements carried out the first day of experiment and subsequently every 24 h (Figure 6a).

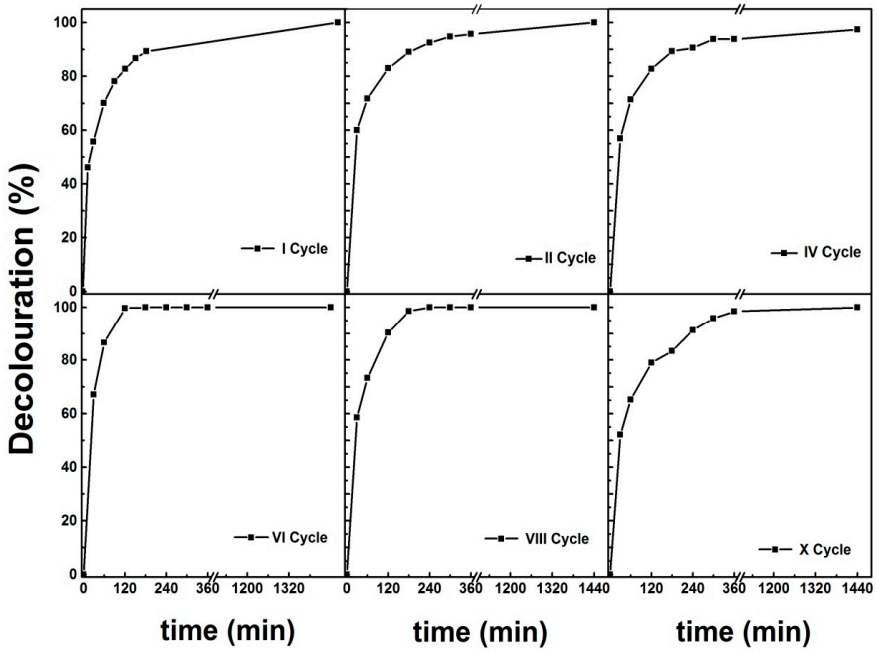

Figure 5. Recycling experiments carried out for the sample PL3d under solar light simulator. The decolouration efficiency of the PL3d coating was investigated for 10 consecutive 24 h cycles using a solar light simulator as radiation source.

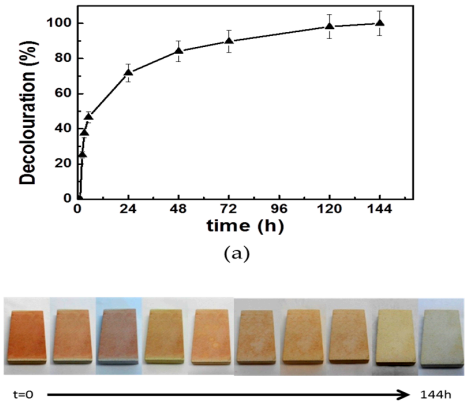

Figure 6. (**a**) Trend of MR decolouration assisted by the sample PL3d in the course of outdoor experiments carried out for one week outdoors. In this period, the humidity was measured in the range of 57%–88% and the weather was partially cloudy. Reported data are presented as mean values ± standard deviation obtained from the analysis of two replicates. (**b**) Pictures of untreated PL3d sample in the time course of outdoor photocatalytic degradation experiment, which point out the progressive decolouration of its surface.

The experimental data revealed that, despite the adverse weather conditions, the MR decolouration percentage increased during the first four days of experiment from 25% to 90% and kept almost constant for the subsequent days of exposure, thus indicating not only a good photoactivity for the sample PL3d, as reported for indoor experiments, but also that the photocatalytic properties are retained during the outdoor exposure.

During the course of the outdoor photocatalysis experiment, the spectroscopic signal associated to the presence of TiO_2 NRs on PL was monitored by reflectance spectroscopy. As reported above in Figure 3b, the presence of TiO_2 NRs on PL is associated with an intense absorption increase in the region below 350 nm. In this spectral region, the MR does not show any absorption peak; therefore, the shoulder below 350 nm can be safely ascribed to TiO_2 NRs (Figure 7b). Therefore, it turns out that in the course of the outdoor experiment the signal associated to TiO_2 NRs stays constant (Figure 7a), thus indicating a stability of the coating under the experimental conditions.

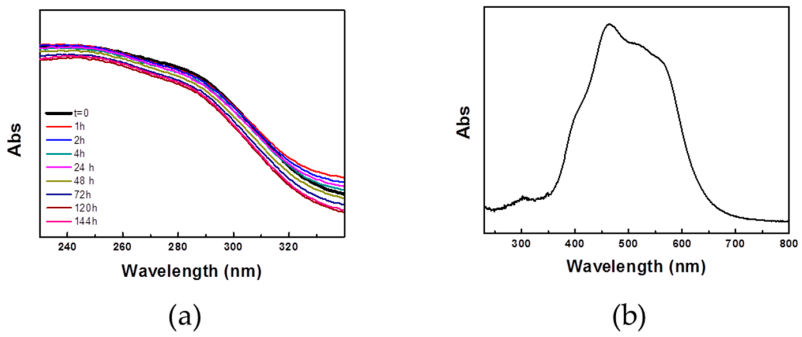

Figure 7. Absorbance spectrum of the sample PL3d (calculated from reflectance measurements) in the course of photocatalysis experiment outdoor. (**a**) Reflectance spectrum in the range of 230–350 nm where the signal of TiO_2 NRs is typically detected. The spectrum shows how the TiO_2 NR signal did not undergo significative variations in the course of experiment, thus suggesting the stability upon outdoor exposition. (**b**) Absorbance spectrum of the PL3d specimen stained with the Methyl Red, acquired using the PL3d sample as reference. The reflectance spectrum highlights that MR does not absorb below 350 nm.

Furthermore, we investigated possible leaching of TiO_2 from the sample PL3d. For this purpose, the sample was immersed in water at pH 6.5 and irradiated by a solar light simulator for 3 h under stirring. Subsequently, the water solution was analysed by Atomic Absorption Spectroscopy (AAS) to detect concentration of Ti species possibly released in water. Ti concentration detected in the experiment was found to be 0.94 µg/L. The PL3d coating was further investigated by measuring the ΔE* after the exposure at UV light for 7.5 h. Samples were irradiated with a 300 W ultraviolet lamp (Sanolux, Radium) with an irradiance value of 25 W/m^2 in the range 280–400 nm. The distance between the samples and the lamp was approximately 40 cm. Experiments result in a ΔE* = 0.98, thus showing that the aesthetic properties of PL surface upon treatment are preserved even when the sample is exposed to UV light. Finally, the durability and the stability in terms of adhesion of the modified TiO_2 NRs on the surface of the stone was tested. In the absence of standard procedures for the evaluation of adhesion of nanostructured coatings on stone, a water impact test was performed according to the procedure reported in Reference [40]. Selected stone samples (PL3c and PL3d) were exposed to a water jet with a diameter of 1 cm, sprayed on the specimen surface at a pressure of 0.2 bar from a distance of 50 cm. The specimen was placed horizontally and impacted by a perpendicular jet on a surface area of approximately 4 cm^2. The test was carried out for 10 min and subsequently the samples were dried in an oven at 60 °C for 18 h. The reflectance spectra of the samples recorded before and after the exposure to the water jet clearly show, in both cases, an increase in the absorbance signal below 350 nm, ascribable to the presence of TiO_2 NRs (data not reported).

In addition, the photocatalytic activity of the PL3c and PL3d samples was evaluated before and after the exposure to the water jet, resulting still photoactive. Remarkably, the decolouration profile with time for both PL3c and PL3d samples, respectively, closely follow the trend recorded for the same samples before the water jet exposure (Figure 8). This result clearly indicates the stability of the TiO_2 NR based coatings, irrespective of the application method. The photocatalytic activity does not appear to undergo to any modification upon exposure of the sample to the water jet under the reported conditions, therefore the observed loss in contact angle value cannot definitely be ascribed to a wash out of TiO_2 NRs present at the surface of the investigated stone.

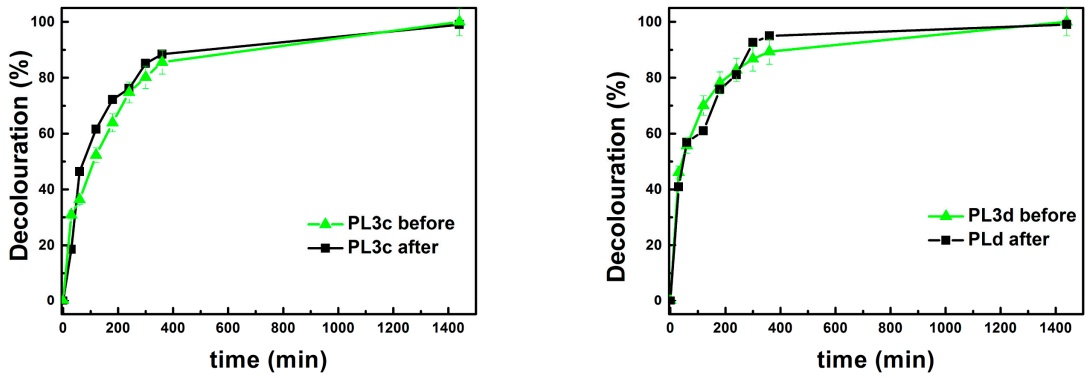

Figure 8. Photocatalytic decolouration of Methyl Red (MR) for: PL3c (**a**); and PL3d (**b**) samples before and after the treatment with a jet of water for 10 min and a subsequent drying for 18 h at 60 °C. The samples were irradiated with a solar light simulator.

The reported results highlighted that the TiO_2 NRs hold a great potential to convey self-cleaning ability and protective properties to complex and unconventional substrates as the PL. In particular, TiO_2 NRs could be used also as additive in suitable polymeric coating, such as those typically employed in the field of restoration.

3. Materials and Methods

3.1. Materials

All chemicals were of the highest purity available and were used as received without further purification. Titanium tetraisopropoxide ($Ti(OiPr)_4$ or TTIP, 99.999%), trimethylamino-*N*-oxide dihydrate ($((CH_3)_3NO{\cdot}2H_2O$ or TMAO, 98%), oleic acid ($C_{18}H_{33}CO_2H$ or OLEA, 90%) and Methyl Red (2-(4-dimethylaminophenylazo)benzoic acid—C.I. 13020, MR) were purchased from Aldrich. All solvents used were of analytical grade and purchased from Aldrich (Milano, Italy).

3.2. Synthesis of TiO_2 NRs

The hydrolysis of titanium tetraisopropoxide (TTIP) into technical grade OLEA at low temperatures (100 °C), thanks to the direct injection of a large volume of aqueous trimethylamino-*N*-oxide dihydrate (TMAO), allowed the synthesis of organic-capped TiO_2 NRs (100% anatase) [32], being the excess of aqueous base solution able to catalyse the poly-condensation. The growth was carried out for 5 days, after which TiO_2 NRs were readily precipitated upon addition of an excess of ethanol. The resulting precipitate was isolated by centrifugation and washed three times with ethanol to remove the excess of surfactant. Finally, the OLEA-coated TiO_2 NRs were easily re-dispersed in $CHCl_3$. The obtained solution resulted clear, without aggregates or suspended matters, thanks to the presence of OLEA as coordinating agent. A detailed structural and morphological characterization of the as-prepared TiO_2 NRs can be found elsewhere [32].

3.3. Application of the Coating on the Stone Samples

Pietra Leccese (PL) samples, having dimensions 5 × 1 × 2.5 cm (l, d, h), were previously thermally treated on a hot plate at 40 °C for 1 h, dried under vacuum for 30 min and finally cleaned by a mild jet of nitrogen to prevent humidity accumulation. Then, the samples were treated with a chloroform dispersion of the as prepared TiO_2 NRs. Two application techniques, namely casting and dipping were tested. In particular, for casting application, defined volumes of TiO_2 NRs dispersion were cast on the stone surface of each sample by using a syringe, to thoroughly cover the surface. Then, the samples were let dry at room temperature. The volume and the concentration of TiO_2 NRs were defined in order to achieve the final amount of TiO_2 NRs per surface unit on the stone, as reported in the Table 1. In particular, for sample PL1c, 150 μL of TiO_2 NRs 0.5 M were deposited, while, in the case of PL2c and PL3c, 1 mL of TiO_2 NRs 0.5 M and TiO_2 NRs 0.05 M, respectively, were cast. The concentration of TiO_2 NRs solutions was determined by atomic absorption spectroscopy, while the amount of TiO_2 NRs per surface unit on the stone was determined by weighing, as reported in Table 1.

The dipping procedure was carried out by immersing the samples in 50 mL of TiO_2 NR dispersed in chloroform, at increasing TiO_2 NR content, as reported in Table 1, for 30 min and then left dry at room temperature overnight. As control experiments, PL samples were treated with OLEA dissolved in $CHCl_3$ by casting 1 mL of OLEA, at a concentration compatible with the amount of oleic acid present in a representative TiO_2 NR treated sample.

3.4. Characterization

3.4.1. Transmission Electron Microscopy

Transmission electron microscopy (TEM) analysis was performed by a JEOL JEM-1011 (JEOL, Akishima, Tokyo, Japan) microscope operating at 100 kV. The TEM samples were prepared drop casting TiO_2 NRs dispersed in $CHCl_3$ onto a carbon TEM grid.

3.4.2. IR-ATR Spectroscopy

Mid-infrared spectra were acquired with a Varian 670-IR spectrometer (Varian Inc, Palo Alto, CA, USA), equipped with a DTGS (deuteratedtryglicinesulfate) detector. The spectral resolution used

for all experiments was 4 cm^{-1}. For Attenuated Total Reflection (ATR) measurements, the internal reflection element (IRE) used was a one bounce 2 mm diameter diamond microprism. Materials were cast directly onto the internal reflection element, by depositing the solution or dispersion of interest (3–5 μL) on the upper face of the diamond crystal and allowing the solvent to evaporate.

3.4.3. UV-Vis Absorption Spectroscopy

UV-Vis absorption spectra and reflectance spectra were recorded with a UV-Vis-near IR Cary 5 (Agilent Technologies, Inc., Santa Clara, CA, USA) (Varian spectrophotometer). For the reflectance spectra, an integrating sphere was used.

3.4.4. Colorimetry

The measure of the colour change was performed with a Minolta CR 300 Chroma Meter reflectance colorimeter (Konica Minolta Inc., Tokyo, Japan) on the specimens measuring 5 × 1 × 5 cm. The chromatic variations due to the application of catalyst were measured in the CIELab space, expressed as [41]:

$$\Delta E^* = \sqrt{(\Delta L^*)^2 + (\Delta a^*)^2 + (\Delta b^*)^2} \quad (1)$$

where $(\Delta L)^{2*}$ represents the change in brightness, and $(\Delta a)^{2*}$ and $(\Delta b)^{2*}$ the changes in hue. Eighteen regions, of a few square millimetres, were examined and averaged on each stone sample.

3.4.5. Static Contact Angle Measurement

Measurements were taken with a Costech contact angle measuring instrument (Costech International S.p.A., Cernusco sul Naviglio, Milan, Italy), according the current European Standard [42].The specimens measuring 5 × 1 × 5 cm were investigated. Ten regions, of a few square millimetres, were examined and averaged on each stone sample.

3.4.6. Water Absorption Test

To evaluate the water absorption, the contact-sponge test was carried out [43] on samples 10 × 2 × 10 cm in dimension. A disc-shaped sponge, having an area of 22.06 cm^2, was soaked with 5 mL of water and pressed against the stone surface for 1 min; water absorption was calculated as:

$$WA = (mi - mf)/(A \times t) \quad (2)$$

where *mi* is the initial weight of the sponge soaked with water, *mf* is the weight of the sponge after the contact, *A* is the sponge area and *t* is the contact time.

The test was performed on the same samples before and after the treatments.

3.4.7. Water Vapour Permeability Test

The water vapour permeability is the mass of water vapour transmitted through stone per area unit in a time unit, under defined conditions, and describes the ability of a material to allow water vapour passing through. Such a parameter indicates the breathability of the stone surface and it is essential for a coating material designed for historical and artistic stonework restoration, which is required to retain the stone capability to let water vapour permeate to the external environment. The permeability to water vapour was evaluated on the samples measuring 5 × 1 × 5 cm, following the procedure described in the Italian Standard [44].The measurements were carried out on the untreated samples and repeated on the same samples, after the treatments.

3.5. Photocatalytic Activity and Self-Cleaning Test

Photocatalytic activity was tested by monitoring the photo-degradation of Methyl Red dye (MR) (Sigma Aldrich, Milano, Italy), both under a solar light simulator and under sunlight in outdoor

experiments. The target molecule was deposited by casting of 100 μL of a 3.5×10^{-3} M solution in isopropanol (3.5×10^{-7} moles, equal to 9.4×10^{-9} mg/cm^2). The solar simulator is a Xenon lamp 150 W, (Oriel Instruments Newport, CA, USA) with irradiance of 0.0455 W/cm^2 (0.33 SUN) measured at the distance where samples were placed during illumination. Each experiment lasted 24 h, during which reflectance spectra were recorded, using the spectrum of the respective sample before dye deposition as baseline, in order to selectively monitor the MR signal and follow the decolouration during the irradiation time.

The percentage of decolouration was calculated through the value of absorbance measured at 460 nm at subsequent times, by the following Equation:

$$\text{decolouration} = \frac{A_0 - A_t}{A_0} \times 100 \quad (3)$$

Outdoor photocatalytic experiments were carried out in the same condition adopted for the indoor experiments, except for the solar irradiation and the exposure to weathering. The experimental data referred to the photocatalytic activity of TiO_2 NR based coatings under solar light simulator irradiation are reported as mean values ± standard deviation obtained from the analysis of three replicates, while experimental data related to photocatalysis experiments carried out outdoor are reported as mean values ± standard deviation obtained from the analysis of two replicates.

4. Conclusions

In this work, oleic acid (OLEA) capped TiO_2 NRs, synthesized by exploiting a colloidal chemistry route, were applied onto a stone material, namely the *Pietra Leccese* (PL), widely used in historical buildings of the cultural heritage of Apulia Region. The treatment with the OLEA capped TiO_2 NRs was found to convey self-cleaning ability and protective properties to the PL stone thanks to the high photocatalytic activity and the hydrophobic surface of the organic capped TiO_2 NRs.

The TiO_2 NRs were deposited on the stone by casting and by dipping and an extensive chemical and physical characterization of the treated surface was performed, revealing that the TiO_2 NR based coatings did not significantly affect the aesthetical characteristics of the investigated stone specimens. Interestingly, TiO_2 NRs were demonstrated to convey a hydrophobic behaviour to the stone, probably due to the presence of oleic acid molecules coordinating the surface of TiO_2 NRs, while leaving unchanged the water vapour permeability of the stone.

For the first time, the photocatalytic activity of TiO_2 NRs was tested at solid–air interface, both under irradiation with a solar light simulator and outdoors using the azo dye Methyl Red as target compound to simulate pollution from organic compounds. Photocatalysis tests showed the high efficiency of TiO_2 NRs in assisting degradation of an organic compound, under the investigated conditions.

In summary, the proposed treatment of PL stone with TiO_2 NR dispersion presents a great potential as photocatalyst at solid–air interface, being a promising candidate as photoactive additive with self-cleaning and hydrophobic ability for product suited to protection of building materials in the context of the cultural heritage.

Clearly, different relevant issues will need to be considered for the translation of the proposed nanostructured materials in the application phase, when issues such as solvent toxicity and long term performance of the final product have to be properly evaluated in field.

Acknowledgments: This work was partially supported by the Apulia Region Funded Projects NanoApulia (MDI6SR) and Cleaning, protection and consolidation of traditional building materials of the Puglia region (PS083), EC-funded 7th FP LIMPID (Grant No. 310177), ReLa VALBIOR, Sens&Micro LAB, and PRIN 2012 (prot. 20128ZZS2H) Italian National projects.

Author Contributions: Angela Calia, Mariateresa Lettieri, Donato Colangiuli and Roberto Comparelli conceived and designed the experiments; Francesca Petronella, Antonella Pagliarulo and Maria Lucia Curri performed the experiments; Marinella Striccoli, Antonella Pagliarulo, Mariateresa Lettieri, Donato Colangiuli and Roberto Comparelli analysed the data; and Roberto Comparelli, Maria Lucia Curri and Angela Calia wrote the paper.

Conflicts of Interest: The authors declare no conflict of interest.

References and Notes

1. Janvier-Badosa, S.; Brunetaud, X.; Beck, K.; Al-Mukhtar, M. Kinetics of Stone Degradation of the Castle of Chambord in France. *Int. J. Arch. Herit.* **2016**, *10*, 96–105. [CrossRef]
2. Ali, H.E.; Khattab, S.A.; Al-Mukhtar, M. *Engineering Geology for Society and Territory—Volume 8: Preservation of Cultural Heritage*; Lollino, G., Giordan, D., Marunteanu, C., Christaras, B., Yoshinori, I., Margottini, C., Eds.; Springer International Publishing: Cham, Switzerland, 2015; pp. 515–520.
3. Sadat-Shojai, M.; Ershad-Langroudi, A. Polymeric coatings for protection of historic monuments: Opportunities and challenges. *J. Appl. Polym. Sci.* **2009**, *112*, 2535–2551. [CrossRef]
4. Favaro, M.; Mendichi, R.; Ossola, F.; Russo, U.; Simon, S.; Tomasin, P.; Vigato, P.A. Evaluation of polymers for conservation treatments of outdoor exposed stone monuments. Part I: Photo-oxidative weathering. *Polym. Degrad. Stab.* **2006**, *91*, 3083–3096. [CrossRef]
5. Chiantore, O.; Lazzari, M. Photo-oxidative stability of paraloid acrylic protective polymers. *Polymer* **2001**, *42*, 17–27. [CrossRef]
6. Pedna, A.; Pinho, L.; Frediani, P.; Mosquera, M.J. Obtaining SiO_2–fluorinated PLA bionanocomposites with application as reversible and highly-hydrophobic coatings of buildings. *Prog. Org. Coat.* **2016**, *90*, 91–100. [CrossRef]
7. Maxová, I.; Slesiger, R.; Kubová, O. Test of some antigraffiti systems for preservation of sandstone monuments. In Proceedings of the 7th European Conference "SAUVEUR", Safeguarded Cultural Heritage, Prague, Czech Republic, 31 May–3 June 2006.
8. Licchelli, M.; Marzolla, S.J.; Poggi, A.; Zanchi, C. Crosslinked fluorinated polyurethanes for the protection of stone surfaces from graffiti. *J. Cult. Herit.* **2011**, *12*, 34–43. [CrossRef]
9. Gómez-Ortíz, N.; De la Rosa-García, S.; González-Gómez, W.; Soria-Castro, M.; Quintana, P.; Oskam, G.; Ortega-Morales, B. Antifungal Coatings Based on $Ca(OH)_2$ Mixed with ZnO/TiO_2 Nanomaterials for Protection of Limestone Monuments. *ACS Appl. Mater. Interfaces* **2013**, *5*, 1556–1565. [CrossRef] [PubMed]
10. Lee, J.; Mahendra, S.; Alvarez, P.J.J. Nanomaterials in the Construction Industry: A Review of Their Applications and Environmental Health and Safety Considerations. *ACS Nano* **2010**, *4*, 3580–3590. [CrossRef] [PubMed]
11. Taurino, R.; Barbieri, L.; Bondioli, F. Surface properties of new green building material after TiO_2–SiO_2 coatings deposition. *Ceram. Int.* **2016**, *42*, 4866–4874. [CrossRef]
12. Pacheco-Torgal, F.; Jalali, S. Nanotechnology: Advantages and drawbacks in the field of construction and building materials. *Constr. Build. Mater.* **2011**, *25*, 582–590. [CrossRef]
13. Chen, J.; Poon, C.-S. Photocatalytic construction and building materials: From fundamentals to applications. *Build. Environ.* **2009**, *44*, 1899–1906. [CrossRef]
14. Herrmann, J.-M. Photocatalysis fundamentals revisited to avoid several misconceptions. *Appl. Catal. B Environ.* **2010**, *99*, 461–468. [CrossRef]
15. Herrmann, J.-M. Heterogeneous photocatalysis: Fundamentals and applications to the removal of various types of aqueous pollutants. *Catal. Today* **1999**, *53*, 115–129. [CrossRef]
16. Cappelletti, G.; Fermo, P.; Camiloni, M. Smart hybrid coatings for natural stones conservation. *Prog. Org. Coat.* **2015**, *78*, 511–516. [CrossRef]
17. Colangiuli, D.; Calia, A.; Bianco, N. Novel multifunctional coatings with photocatalytic and hydrophobic properties for the preservation of the stone building heritage. *Constr. Build. Mater.* **2015**, *93*, 189–196. [CrossRef]
18. La Russa, M.F.; Rovella, N.; Alvarez de Buergo, M.; Belfiore, C.M.; Pezzino, A.; Crisci, G.M.; Ruffolo, S.A. Nano-TiO_2 coatings for cultural heritage protection: The role of the binder on hydrophobic and self-cleaning efficacy. *Prog. Org. Coat.* **2016**, *91*, 1–8. [CrossRef]

19. Pinho, L.; Rojas, M.; Mosquera, M.J. Ag–SiO_2–TiO_2 nanocomposite coatings with enhanced photoactivity for self-cleaning application on building materials. *Appl. Catal. B Environ.* **2015**, *178*, 144–154. [CrossRef]
20. Bergamonti, L.; Alfieri, I.; Franzò, M.; Lorenzi, A.; Montenero, A.; Predieri, G.; Raganato, M.; Calia, A.; Lazzarini, L.; Bersani, D.; et al. Synthesis and characterization of nanocrystalline TiO_2 with application as photoactive coating on stones. *Environ. Sci. Pollut. Res.* **2014**, *21*, 13264–13277. [CrossRef] [PubMed]
21. Pinho, L.; Elhaddad, F.; Facio, D.S.; Mosquera, M.J. A novel TiO_2–SiO_2 nanocomposite converts a very friable stone into a self-cleaning building material. *Appl. Surf. Sci.* **2013**, *275*, 389–396. [CrossRef]
22. Kapridaki, C.; Pinho, L.; Mosquera, M.J.; Maravelaki-Kalaitzaki, P. Producing photoactive, transparent and hydrophobic SiO_2-crystalline TiO_2 nanocomposites at ambient conditions with application as self-cleaning coatings. *Appl. Catal. B Environ.* **2014**, *156–157*, 416–427. [CrossRef]
23. Pinho, L.; Mosquera, M.J. Titania-Silica Nanocomposite Photocatalysts with Application in Stone Self-Cleaning. *J. Phys. Chem. C* **2011**, *115*, 22851–22862. [CrossRef]
24. Petronella, F.; Truppi, A.; Ingrosso, C.; Placido, T.; Striccoli, M.; Curri, M.L.; Agostiano, A.; Comparelli, R. Nanocomposite materials for photocatalytic degradation of pollutants. *Catal. Today* **2016**. [CrossRef]
25. Comparelli, R.; Fanizza, E.; Curri, M.L.; Cozzoli, P.D.; Mascolo, G.; Passino, R.; Agostiano, A. Photocatalytic degradation of azo dyes by organic-capped anatase TiO_2 nanocrystals immobilized onto substrates. *Appl. Catal. B Environ.* **2005**, *55*, 81–91. [CrossRef]
26. Panniello, A.; Curri, M.L.; Diso, D.; Licciulli, A.; Locaputo, V.; Agostiano, A.; Comparelli, R.; Mascolo, G. Nanocrystalline TiO_2 based films onto fibers for photocatalytic degradation of organic dye in aqueous solution. *Appl. Catal. B Environ.* **2012**, *121–122*, 190–197. [CrossRef]
27. Petronella, F.; Curri, M.L.; Striccoli, M.; Fanizza, E.; Mateo-Mateo, C.; Alvarez-Puebla, R.A.; Sibillano, T.; Giannini, C.; Correa-Duarte, M.A.; Comparelli, R. Direct growth of shape controlled TiO_2 nanocrystals onto SWCNTs for highly active photocatalytic materials in the visible. *Appl. Catal. B Environ.* **2015**, *178*, 91–99. [CrossRef]
28. Petronella, F.; Fanizza, E.; Mascolo, G.; Locaputo, V.; Bertinetti, L.; Martra, G.; Coluccia, S.; Agostiano, A.; Curri, M.L.; Comparelli, R. Photocatalytic Activity of Nanocomposite Catalyst Films Based on Nanocrystalline Metal/Semiconductors. *J. Phys. Chem. C* **2011**, *115*, 12033–12040. [CrossRef]
29. D'Arienzo, M.; Carbajo, J.; Bahamonde, A.; Crippa, M.; Polizzi, S.; Scotti, R.; Wahba, L.; Morazzoni, F. Photogenerated Defects in Shape-Controlled TiO_2 Anatase Nanocrystals: A Probe to Evaluate the Role of Crystal Facets in Photocatalytic Processes. *J. Am. Chem. Soc.* **2011**, *133*, 17652–17661. [CrossRef] [PubMed]
30. Chen, X.; Mao, S.S. Titanium Dioxide Nanomaterials: Synthesis, Properties, Modifications, and Applications. *Chem. Rev.* **2007**, *107*, 2891–2959. [CrossRef] [PubMed]
31. Fittipaldi, M.; Curri, M.L.; Comparelli, R.; Striccoli, M.; Agostiano, A.; Grassi, N.; Sangregorio, C.; Gatteschi, D. A Multifrequency EPR Study on Organic-Capped Anatase TiO_2 Nanocrystals. *J. Phys. Chem. C* **2009**, *113*, 6221–6226. [CrossRef]
32. Cozzoli, P.D.; Kornowski, A.; Weller, H. Low-Temperature Synthesis of Soluble and Processable Organic-Capped Anatase TiO_2 Nanorods. *J. Am. Chem. Soc.* **2003**, *125*, 14539–14548. [CrossRef] [PubMed]
33. Normal 1/88 "Alterazioni macroscopiche dei materiali lapidei: lessico". Italian Regulation.
34. Bonanni, P.; Cacace, C.; Giovagnoli, A.; Gaddi, R. *L'impatto Dell'inquinamento Atmosferico Sui Beni di Interesse Storico-Artistico Esposti All'aperto*; APAT—Servizio Stampa ed Editoria: Roma, Italy, 2006; Volume 1.
35. Lettieri, M.; Calia, A.; Licciulli, A.; Marquardt, A.E.; Phaneuf, R.J. Nanostructured TiO_2 for stone coating: Assessing compatibility with basic stone's properties and photocatalytic effectiveness. *Bull. Eng. Geol. Environ.* **2015**, 1–14. [CrossRef]
36. Kronlund, D.; Bergbreiter, A.; Meierjohann, A.; Kronberg, L.; Lindén, M.; Grosso, D.; Smått, J.-H. Hydrophobization of marble pore surfaces using a total immersion treatment method—Product selection and optimization of concentration and treatment time. *Prog. Org. Coat.* **2015**, *85*, 159–167. [CrossRef]
37. Dumée, L.; Germain, V.; Sears, K.; Schütz, J.; Finn, N.; Duke, M.; Cerneaux, S.; Cornu, D.; Gray, S. Enhanced durability and hydrophobicity of carbon nanotube bucky paper membranes in membrane distillation. *J. Membr. Sci.* **2011**, *376*, 241–246. [CrossRef]
38. Mosquera, M.J.; Benítez, D.; Perry, S.H. Pore structure in mortars applied on restoration: Effect on properties relevant to decay of granite buildings. *Cem. Concr. Res.* **2002**, *32*, 1883–1888. [CrossRef]

39. Mascolo, G.; Comparelli, R.; Curri, M.L.; Lovecchio, G.; Lopez, A.; Agostiano, A. Photocatalytic degradation of methyl red by TiO_2: Comparison of the efficiency of immobilized nanoparticles versus conventional suspended catalyst. *J. Hazard. Mater.* **2007**, *142*, 130–137. [CrossRef] [PubMed]
40. Calia, A.; Lettieri, M.; Masieri, M. Durability assessment of nanostructured TiO_2 coatings applied on limestones to enhance building surface with self-cleaning ability. *Build. Environ.* **2016**, *110*, 1–10. [CrossRef]
41. *15886, U.E. Conservation of Cultural Property—Test Methods—Colour Measurement of Surfaces*; BSI Group: London, UK, 2010.
42. *15802, U.E. Conservation of Cultural Property—Test Methods—Determination of Static Contact Angle*; BSI Group: London, UK, 2010.
43. *UNI 11432 Cultural Heritage—Natural and Artificial Stone—Determination of the Water Absorption by Contact Sponge*; Ente Italiano di Normazione: Milan, Italy, 2011.
44. *NORMAL Rec. 21/85 Permeabilità al Vapor D'acqua*; CNR/ICR: Rome, Italy, 1985. (In Italian)